Mixture of piperazine and potassium carbonate to absorb CO_2 in the packed column: modelling study

Tohid N.Borhani[a*], Shervan Babamohammadi[b], Navid Khallaghi[c], Zhein Zhang[d]

[a]School of Engineering, Division of Chemical Engineering, University of Wolverhampton, Wolverhampton, WV1 1LY, UK

[b]Chemical Engineering Department, Faculty of Engineering, University Malaya, 50603 Kuala Lumpur, Malaysia

[c]Department of Chemical Engineering and Analytical Science, University of Manchester, Manchester, M13 9PL, UK

[d]William G. Lowrie Department of Chemical and Biomolecular Engineering, The Ohio State University, Columbus, OH 43210, USA

Abstract:

A rate-based non-equilibrium model is developed for CO_2 absorption with the mixture of piperazine and potassium carbonate solution. The model is based on the mass and heat transfer between the liquid and the gas phases on each packed column segment. The thermodynamic equilibrium assumption (physical equilibrium) is considered only at the gas-liquid interface and chemical equilibrium is assumed in the liquid phase bulk. The calculated mass transfer coefficient from available correlations is corrected by the enhancement factor to account for the chemical reactions in the system. The Extended-UNIQUAC model is used to calculate the non-idealities related to the liquid phase, and the Soave-Redlich-Kwong (SRK) equation of state is used for the gas phase calculations. The thermodynamic analysis is also performed in this study. The enhancement factor is used to represent the effect of chemical reactions of the piperazine promoted potassium carbonate solution, which has not been considered given the rigorous electrolyte thermodynamics in the absorber. The developed model showed good agreement with the experimental data and similar studies in the literature.

Keywords: Amine mixture; CO_2 capture; Absorption; Rate-based model; Extended-UNIQUAC.

1. Introduction

Chemical absorption is known as the most developed technique for CO_2 separation [1]. Utilising an optimal solvent with a high loading capacity, high stability, low regeneration energy, and fast reaction rates can improve the absorption process. For the chemical adsorption of CO_2, a

* Corresponding author: t.borhani@wlv.ac.uk and tohid.n.borhani@gmail.com

multitude of solvents is commonly used which include solutions of amine, ammonia, carbonate, hydroxide, and alkanolamine salt solutions [2]. Although single component solutions are most utilised in absorbing carbon dioxide, mixtures of different components can be used to enhance the absorption capacity. This study aims to address the absorption of CO_2 in mixtures of an amine, piperazine (PZ), in salt solutions of potassium carbonate. Prior to describing the model used in this study, a review of CO_2 absorption in different amines is presented to highlight the significance of piperazine, potassium carbonate mixtures as compared with other commonly used solvents.

1.1. Single Amine Solutions

Alkanolamines [3] are the most famous chemical solvents used for CO_2 absorption. There have been many studies focusing on the chemistry, reaction kinetics, thermodynamic or process modelling of CO_2 absorption in amine solutions in the different types of unit operations such as trayed columns, packed columns with different packings, and rotating packed bed (RPB).
Different alkanolamines have different absorption behaviour, with primary or secondary amines having fast reactivity and absorption. On the contrary, tertiary, or sterically hindered amines (SHA) show high absorption equilibrium capacity and low solvent stripping cost. Monoethanolamine (MEA) and methyldiethanolamine (MDEA) are some of the most frequently used commercial amines in the chemical industry. The higher reaction rate of MEA with CO_2 compared to other amines, along with its low cost and low operating pressure requirement makes MEA a significant solvent used in the industry [4,5]. Although MDEA has lower reactivity performance in comparison with MEA, it can provide advantages by having higher CO_2 loading capacity, low heat of regeneration and high CO_2 absorption [6]. However, in terms of heat of absorption, diethanolamine (DEA) is reported to have better performance than the aforementioned alkanolamines [7]. In addition to these standard absorption solvents that are used as single-component solutions, PZ and 2-amino-1-methyl2-propanol (AMP) are also used as chemical absorbents for the CO_2 chemical absorption process. Larger alkanolamine solution can also be used, however, unlike the above-stated amines, triethanolamine (TEA) and diisopropanolamine (DIPA) are more often used in mixed solvent solutions [7].
PZ is a cyclic amine that has shown acceptable absorption capacity even in concentrated conditions [8]. PZ has low vapour pressure, good promoting performance, low degradation and low corrosivity. It has also strong thermal stability, allowing it to be employed at temperatures up to 150 °C, which is significantly greater than the usually used upper limit of 120 °C for MEA. However, solids can be formed at a combination of relatively low temperatures and CO_2

loading (below 0.6 mol CO_2 per mol PZ at 0 °C), and a high CO_2 loading (above 0.9 mol CO_2 per mol PZ). This problem is considered as the main disadvantage of this amine [9].

In comparison with PZ, the AMP solution has a higher CO_2 absorption rate and capacity, being in the same order of magnitude as the MDEA solution, with 1 mol of CO_2 being absorbed by 1 mol amine. Moreover, AMP has lower energy consumption in regeneration, brilliant selectivity, higher resistance to degradation, and a lower corrosion rate compared with the conventional amines mentioned [10].

1.2. Blended Amine Solutions

To enhance the absorption process, aqueous blends of amines have been extensively studied in the literature. One common approach is blending MEA with MDEA, a mixture that exploits the high absorption rate of MEA and the high equilibrium capacity of MDEA [11].

Aqueous mixtures of PZ and MDEA have also been used in industrial operations, albeit to a limited degree [12]. This mixture is known as activated methyldiethanolamine (aMDEA) [13]. As mentioned before, PZ is a cyclic symmetric diamine and contains two amino groups, each mole of PZ is theoretically able to remove two moles of CO_2 and PZ may intensify the fast creation of carbamates. CO_2 reacts with PZ to make zwitterions, which are then deprotonated to produce PZ-carbamate, and CO_2 is quickly transferred to MDEA. PZ can be thought of as a catalyst that accelerates the rate of CO_2 and MDEA reactions [14]. Other benefits of using PZ in the mixture with MDEA include increased resistance to oxidation and thermal degradation. Using MDEA with PZ is also beneficial given that MDEA has resistance to degradation, is suitable for application in concentrations up to 60 wt%, is not corrosive and there is minimal solvent loss [6].

For blends of AMP, Choi et al [15] mixed AMP with hexamethylenediamine (HMDA), MDEA, and PZ separately. The authors reported that the addition of HMDA showed the most enhancement in the reaction rate of AMP. This study has been further extended by studying the blend under three different concentrations of MDEA+AMP at three different temperatures [10]. The results showed that increasing AMP concentration can improve the absorption capacity of the MDEA aqueous solution. The mixture of AMP and PZ is known as CESAR-1. This mixture requires approximately 25% less heat for regeneration than MEA, which was previously used as a reference solvent and has a high resistance to degradation. The cost of implementing CESAR1 in coal-fired power plants was previously estimated at 17% compared to the advanced MEA process [16].

In addition to the above-mentioned amines mixtures, in a study [17], 1-dimethylamino-2-propanol (1DMA2P) and MEA were mixed, and the equilibrium solubility of CO_2 in the mixture was experimentally reported for the first time. The results showed that the increment in the blend mole ratio of 1DMA2P/MEA results in higher CO_2 absorption capacity. A blend ratio of 4/1 (1DMA2P/MEA) showed the highest CO_2 absorption capacity of 0.9342 mol CO_2/mol amine at 181.5 KPa. Conway et al. [18] worked on CO_2 absorption at 40 °C into aqueous solutions of Benzylamine (BZA), and the mixture of BZA contain MEA and 2-Amino-2-methyl-1-propanol (AMP) as the second amine components, respectively. They found the mixture containing BZA/MEA and BZA/AMP demonstrated significantly faster absorption rates in CO_2 loaded solutions up to 0.3 (mol CO_2 per mol MEA) than in unblended MEA solutions at similar alkalinity. From their data, K_G values for the BZA/AMP blend are some ~75% larger than the blend containing MEA/AMP. Gao et al. [19] also formulated a blend by mixing N, N-Diethylethanolamine (DEEA) and piperazine (PZ). They investigated absorption rate, cyclic CO_2 capacity and regeneration rate for 2 mol/L DEEA/PZ with various molar ratios at 313.15 K and 353.15 K in a hollow fibre membrane contactor. They revealed that the higher CO_2 absorption rate and desorption rate and the highest cyclic CO_2 capacity of 0.8540 mol CO_2/L occur when they use the DEEA/PZ solution with the molar ratio of 1.50:0.50. In another study [20], the same authors investigated the equilibrium and kinetics of CO_2 absorption into blends of DEEA and PZ, N-(2aminoethyl) ethanolamine (AEEA) and 1,6-hexamethyl diamine (HMDA), and indicating the CO_2 absorption rates for the mixtures are much higher than that of DEEA. Another application of amines blends could be seen in non-energy industrial processes (e.g., lime kiln process) that the exhausted CO_2 is in high concentration and at high temperature. Nwaoha et al. [21] studied CO_2 capture from the lime kiln by using 1,5–diamino–2–methylpentane (DAMP) blended with AMP. They revealed that in comparison with the single MEA solvent, the AMP-DA2MP blend shows higher CO_2 absorption efficiency (up to 36.17%), higher $K_G av_{(ave)}$(up to 65.85%), higher $K_L av$ (up to 28.29%) and lower Q_{reg} (up to 32.54%). Hamidi et al. [22] have investigated the CO_2 solubility and regeneration of aqueous solution of MDEA and MEA mixed by DAMP. They used an isothermal batch reactor at various MDEA to MEA ratios and DAMP concentration. Results showed that the absorption rate and capacity of the base solution are directly proportional to the DAMP concentration in the sample.

1.3. Amine Promoted Potassium Carbonate Solution

The potassium carbonate solution is a promising alternative to amine solutions that showed many advantages, mainly because of its low regeneration energy, low degradation rates and low

corrosivity [23]. However, a particular disadvantage of using these mixtures is the low reaction rate of K_2CO_3 with CO_2. This can be ameliorated by the addition of other components as promoters. One prevalent approach is the addition of amines as promoters to improve its performance and effectiveness [3]. Hu et al. [24] reviewed and summarised different amines mixed with potassium carbonate solutions for CO_2 absorption. They revealed that, although MEA promoted potassium carbonate is known as a well-established promoted solution for CO_2 absorption, the high regeneration energy requirement, the degradation, and corrosion issues are still extant as a result of MEA. It is illustrated that adding a small amount of DEA (2–5 wt.%) results in an overly increase in the CO_2 absorption rate into potassium carbonate. Moreover, the DEA promoted potassium carbonate solution has been demonstrated to have a good performance in post-combustion CO_2 capture application in a tray column [25]. Bhosale et al. [26] studied the absorption of CO_2 in the aqueous blend of potassium carbonate, Ethylaminoethanol, and N-methyl-2-Pyrollidone (called Aqueous Potassium Carbonate Ethylaminoethanol N-methyl-2Pyrollidone (APCEN) solvent). In their study, the absorption rate of CO_2 in the APCEN solvent was 18.8% higher than the APCE solvent (aqueous potassium carbonate promoted by Ethylaminoethanol) at 303 K. Another research by Mondal et al. [27] tested aqueous bis(3-aminopropyl) amine known as Dipropylenetriamine (DPTA) and its mixture with MEA, MDEA, AMP and K_2CO_3. They revealed that the (DPTA + K_2CO_3) mixture is superior among other mixtures regarding the loading capacity, enthalpy, and viscosity.

Mixtures of PZ and potassium carbonate is reported as a promising solvent for CO_2 absorption [28]. Cullinane and Rochelle [29] used 0.6 m piperazine as an additive in 20–30 wt% potassium carbonate in the wetted wall column at 40-80 ^oC. The addition of 0.6 m piperazine to 20 wt% potassium carbonate increased the rate of CO_2 absorption and the heat of absorption from 3.7 to 10 kcal/mol. Hilliard and Rochelle [30] modelled the thermodynamics of the mixture of PZ and K_2CO_3 using E-NRTL thermodynamic model in Aspen Plus. They obtained the binary adjustable parameters for this mixture. Cullinane and Rochelle [31] reported that under typical experimental conditions, concentrated K+/PZ mixtures have absorption rates that are 2-3 times faster than 5 M MEA at constant $P^*_{CO_2}$. In another study, Cullinane et al. [32] illustrated that 5 m K+/2.5 m PZ (mol/kg water), provides CO_2 solubility and capacity comparable to 7m (30 wt%) MEA. The heat of CO_2 absorption is less than that in MEA solutions (22 kcal/mol) and decreases from 16 to 9 kcal/mol as temperature increases from 40 to 80 °C and rich CO_2 vapour pressure increases from 100 to 5000 Pa. This decrease in heat of CO_2 absorption, which should reduce the heat requirement for stripping. They also reported that the rate of CO_2 absorption is 1 to 5 times faster than into 7 m MEA.

1.4. Novel Contribution of This Study

In this study, a systematic framework has been developed to model CO_2 absorption using mixtures of PZ + K_2CO_3 solution in a packed column with different compositions. The systematic framework can be used for any other chemical solvents. The Extended UNIQUAC thermodynamic model is used to perform the thermodynamic calculation of the system. Experimental data extracted from literature are extracted to find out the required parameters of the Extended UNIQUAC thermodynamic model. In addition to thermodynamic modelling and analysis, a process model using different mixtures of PZ and Potassium Carbonate for CO_2 absorption is developed in this study. Experimental pilot plant data from literature [33] are used to validate the process model. These data are CO_2 absorption in two different mixtures 5 m (mol/kg H_2O) K^+ + 2.5 m PZ and 6.4 m K_+ + 1.6 m PZ using two different types of packings in the absorber column. The performance of the solvent is discussed in the simulated absorber column. In addition to modelling the column, thermodynamic modelling of CO_2 absorption in PZ + K_2CO_3 is presented.

2. Model development

A general framework for mathematical modelling of the CO_2 absorption process (Figure 1) is developed. This modelling framework can be used for any chemical absorption process and helps to generate a specific model describing CO_2 absorption using piperazine-promoted potassium carbonate solution.

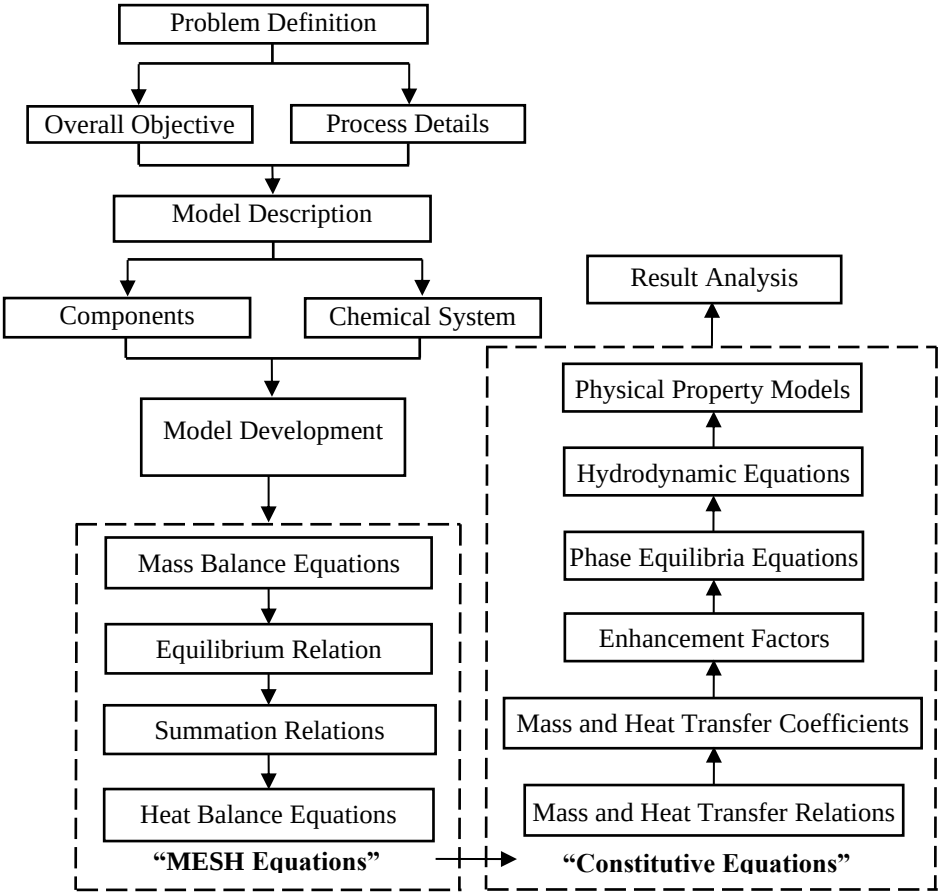

Figure 1: Schematic diagram of systematic modelling framework of the CO_2 absorption process.

As shown in Figure 1, the specific model generation procedure consists of four main steps: Problem definition, Model description, Model construction and solution, Model validation, and analysis. The modelling framework starts with the problem definition in terms of the overall modelling objectives and details of the process to be studied. The overall objective of this modelling is the utilisation of the Extended UNIQUAC thermodynamic model in the development of a non-equilibrium rate-based mathematical model for the absorber of piperazine promoted potassium carbonate process as well as using the enhancement factor to account for the effects of the chemical reaction on the CO_2 capturing by PZ promoted potassium carbonate process. Also, the performance of this solvent in capturing CO_2. This mathematical model considers the effects of chemical reactions, phase equilibria, and column hydrodynamics on the mass and heat transfer between vapour and liquid phases.

The process details could be operational characteristics/assumptions such as steady versus unsteady state, equilibrium versus non-equilibrium, adiabatic versus non-adiabatic. The main assumptions in the process should be considered in this step as follow:

- Chemical equilibrium among the reacting species in the liquid phase is assumed in the liquid phase bulk.
- Axial dispersion is not considered.
- The interfacial surface area is the same for heat and mass transfer (complete wetting of the tray or packing is assumed).
- The absorption column is adiabatic (well-insulated).
- The condition is steady state.
- The pressure drop across the trays is negligible.
- Only carbon dioxide and water will diffuse from the gas phase to the liquid phase.

The model description step in the framework is related to introducing the components and species of the system. The thermodynamic method (activity coefficient model), which account for the effects on non-idealities, is considered in this step. There are numerous data issues to be identified that are of immediate use in the model construction, as well as used in the longer-term issue of model validation.

This study deals with one gas stream and one liquid stream (PZ promoted potassium carbonate solution), with the two streams being at contact in order to transfer the CO_2 from the gas stream to the liquid solution. In the systems under study, there are CO_2, K_2CO_3, $KHCO_3$, PZ, and H_2O. Then according to these components, the species such as K^+, HCO_3^-, CO_3^{2-}, H^+, OH^-, H_2O, CO_2, PZ, $PZCOO^-$, PZH^+, PZH_2^{2+}, H^+PZCOO^-, $PZ(COO^-)_2$ should be considered in the electrolyte system.

The model construction and solution are concerned with listing the necessary equations for the process model and solving them using an appropriate strategy. The appropriate modelling of the reactive absorption column depends on the proper selection of column internals, sufficient knowledge of the process behaviour, and details about the column's design. By using the approach used by Krishnamurthy and Taylor [34] and according to Figure 1, the rate-based model for the PZ-promoted potassium carbonate process in a packed column is developed. In non-equilibrium rate-based modelling, the MERQ equations must be considered for the system under study. The MERQ equations (**M**ass balance equations; **E**nergy balance equations; **R**ate (Transfer rate) equations; e**Q**uilibrium relations) are composed of MESH equations (**M**ass balance equations; **E**quilibrium relation; **S**ummation relations; **E**nthalpy balance equations) and some more equations (namely transfer rates, transfer coefficients, chemical reactions, phase equilibria, hydrodynamic equations, and physical properties of the chemical systems which can be found in the literature and textbooks). To have more clear information about the required

equations for this modelling the flowing list can be considered for a non-equilibrium rate-based model with enhancement factor:

- Material/mass balance
- Equilibrium relations
- Summation equations
- Enthalpy/heat balances
- Mass transfer relations
- Heat transfer relations
- Reaction kinetics (Enhancement factor)
- Phase equilibria relations
- Hydrodynamic relations

2.1. Model Equations

All of the above-mentioned equations of the model are presented in the following subsections:

2.1.1. The MESH equations

Mass balance equations, **E**quilibrium relation, **S**ummation relations, and **H**eat (Enthalpy) balance equations) are the governing equations of the CO_2 absorption model and are summarised in Table 1.

Table 1: Main governing equations of the model (mass balance, equilibrium relation, summation relations, and heat balance).

Mass Balance for Gas and Liquid Phases	
$\frac{dG}{dz} = -\left(N_{CO_2} + N_{H_2O}\right)a_w A_c$	(1)
$G\frac{dy_{CO_2}}{dz} = -y_{CO_2}\frac{dG}{dz} - N_{CO_2}a_w A_c = N_{H_2O}y_{CO_2}a_w A_c - N_{CO_2}\left(1 - y_{CO_2}\right)a_w A_c$	(2)
$G\frac{dy_{H_2O}}{dz} = -y_{H_2O}\frac{dG}{dz} - N_{H_2O}a_w A_c = N_{CO_2}y_{H_2O}a_w A_c - N_{H_2O}\left(1 - y_{H_2O}\right)a_w A_c$	(3)
$\frac{dL}{dz} = -N_{H_2O}a_w A_c$	(4)
$L\frac{dx_{CO_2}}{dz} = -x_{CO_2}\frac{dL}{dz} - N_{CO_2}a_w A_c = \left(N_{H_2O}x_{CO_2} - N_{CO_2}\right)a_w A_c$	(5)
$L\frac{dx_{H_2O}}{dz} = -x_{H_2O}\frac{dL}{dz} + \left(N_{CO_2} - N_{H_2O}\right)a_w A_c = \left(N_{CO_2} - N_{H_2O}\left(1 - x_{H_2O}\right)\right)a_w A_c$	(6)
$L\frac{dx_{K_2CO_3}}{dz} = -x_{K_2CO_3}\frac{dL}{dz} + N_{CO_2}a_w A_c = \left(N_{H_2O}x_{K_2CO_3} + N_{CO_2}\right)a_w A_c$	(7)
$L\frac{dx_{KHCO_3}}{dz} = -x_{KHCO_3}\frac{dL}{dz} - 2N_{CO_2}a_w A_c = \left(N_{H_2O}x_{KHCO_3} - 2N_{CO_2}\right)a_w A_c$	(8)
$L\frac{dx_{PZ}}{dz} = -x_{PZ}\frac{dL}{dz} - N_{CO_2}a_w A_c = \left(N_{H_2O}x_{PZ} - N_{CO_2}\right)a_w A_c$	(9)
$L\frac{dx_{PZH^+}}{dz} = -x_{PZH^+}\frac{dL}{dz} - N_{CO_2}a_w A_c = \left(N_{H_2O}x_{PZH^+} - N_{CO_2}\right)a_w A_c$	(10)

$$L\frac{dx_{PZCOO^-}}{dz} = -x_{PZCOO^-}\frac{dL}{dz} - N_{CO_2}a_wA_c = \left(N_{H_2O}x_{PZCOO^-} - N_{CO_2}\right)a_wA_c \quad (11)$$

Equilibrium Relation

$$y_{i,j} = K_{i,j} \cdot x_{i,j} \quad (12)$$

Summation Relations

$$\sum_{i=1}^{N} y_{i,j} = 1 \text{ and } \sum_{i=1}^{N} x_{i,j} = 1 \quad (13)$$

Heat Balance for Gas and Liquid Phases

$$GC_{P_G}\frac{dT_G}{dz} = \left(N_{CO_2} + N_{H_2O}\right)a_wA_cC_{P_G}T_G - \left(N_{CO_2}C_{P_{CO_2}} + N_{H_2O}C_{P_{H_2O}}\right)a_wA_cT_G - qa_wA_c \quad (14)$$

$$LC_{P_L}\frac{dT_L}{dz} = \left(N_{CO_2}C_{P_{CO_2}} + N_{H_2O}C_{P_{H_2O}}\right)a_wA_c(T_L - T_G) - qa_wA_c + \left(N_{CO_2}\Delta H_{CO_2} + N_{H_2O}\Delta H_{H_2O}\right)a_w \quad (15)$$

2.1.2. Mass and Heat Transfer Relations

From the two-film theory, the rate of CO_2 absorption into potassium carbonate solution can be expressed as follow:

$$N_{\mathrm{CO_2}} = K_{\mathrm{G_{CO_2}}}\left(P_{\mathrm{CO_2}} - P^*_{\mathrm{CO_2}}\right) \quad (16)$$

$P_{\mathrm{CO_2}}$ is the partial pressure of CO_2 in the gas bulk and $P^*_{\mathrm{CO_2}}$ is the equilibrium partial pressure of CO_2 corresponding to its concentration in the liquid bulk. It is noteworthy that $P_{\mathrm{CO_2}} - P^*_{\mathrm{CO_2}}$ is the driving force for mass transfer. The estimation of liquid side resistance to mass transfer requires knowledge of the effect of chemical reactions on mass transfer. Using the rigorous thermodynamic model (Extended UNIQUAC) the $\mathrm{P^*_{CO_2}}$ is calculated. $\mathrm{K_{G_{CO_2}}}$ is the overall gas-phase mass transfer coefficient of carbon dioxide and represents the resistance to mass transfer:

$$\frac{1}{K_{\mathrm{G_{CO_2}}}} = \frac{1}{k_{\mathrm{G_{CO_2}}}} + \frac{H_{\mathrm{e,CO_2}}}{\mathrm{E_{CO_2}}k_{\mathrm{L_{CO_2}}}} \quad (17)$$

This equation consists of two terms; one is the gas phase resistance ($1/k_{\mathrm{G_{CO_2}}}$) and the other is the liquid phase resistance ($H_{\mathrm{CO_2}}/E_{\mathrm{CO_2}}k_{\mathrm{L_{CO_2}}}$). $\mathrm{H_{CO_2}}$ is Henry's law constant for the CO_2, K_2CO_3 system (atm m^3/kmol). Another mass transfer flux that can be considered here is $\mathrm{N_{H_2O}}$. It can be assumed that there is no liquid side mass transfer resistance of the solvent to water vapour. Then the overall mass transfer coefficient for water is as follow:

$$N_{\mathrm{H_2O}} = K_{\mathrm{G_{H_2O}}}\left(P_{\mathrm{H_2O}} - P^{*}_{\mathrm{H_2O}}\right) \quad (18)$$

The heat transfer rate is given by the following equation:

$$q = h_G(T_G - T_L) \quad (19)$$

2.1.3. Mass and Heat Transfer Coefficients

There are several correlations for calculating the mass transfer coefficients and the effective area in columns. In this study, we are dealing with a packed column, and then the random and structured packing must be considered. The available correlations are different from each other in terms of accuracy, limitations, and applicability for a specific system [35]. The correlation of mass transfer presented by Bravo and Fair [36] is used. In addition, the interfacial area correlations were selected corresponding to the mass transfer coefficient model.

$$\begin{aligned} k_G &= 5.23\left(\frac{G}{a_{\mathrm{p}}\mu_G}\right)^{0.7}(Sc_G)^{1/3}\left(a_{\mathrm{p}}d_{\mathrm{p}}\right)^{-2}\left(\frac{a_{\mathrm{p}}D_G}{RT_G}\right) \\ k_L &= 0.0051\left(\frac{L}{a_{\mathrm{w}}\mu_L}\right)^{2/3}(Sc_L)^{-1/2}\left(a_{\mathrm{p}}d_{\mathrm{p}}\right)^{0.4}\left(\frac{\mathrm{g}D_L}{\rho_L}\right) \\ a_{\mathrm{w}} &= a_{\mathrm{p}}\left\{19.78\left(\frac{\rho_G U_G}{a_{\mathrm{p}}\mu_G}\right)^{0.392}\left(\frac{\mu_L U_L^2}{\sigma_L}\right)^{0.392}\left(\frac{\sigma_L^{0.5}}{Z^{0.4}}\right)\right\} \end{aligned} \quad (20)$$

2.1.4. Reaction Effects on Rate Based Modelling

In order to account for the effects of the reactions on the rate-based model, the reaction rate constants (to account for the equilibrium reactions) and enhancement factors (to account for the kinetic reactions) were implemented in this systematic framework.

2.1.4.1. Equilibrium Reactions

When CO_2 is being absorbed in the aqueous solution of potassium carbonate, the following equilibrium reactions must be considered in the liquid aqueous phase:

$$2\mathrm{H_2O(aq)} \overset{\mathrm{K_I}}{\leftrightarrow} \mathrm{OH^-(aq) + H_3O^+(aq)} \quad (R.1)$$

$$\mathrm{CO_2(aq) + 2H_2O(aq)} \overset{\mathrm{K_{II}}}{\leftrightarrow} \mathrm{HCO_3^-(aq) + H_3O^+(aq)} \quad (R.2)$$

$$\mathrm{HCO_3^-(aq) + H_2O(aq)} \overset{\mathrm{K_{III}}}{\leftrightarrow} \mathrm{CO_3^{2-}(aq) + H_3O^+(aq)} \quad (R.3)$$

When PZ is added to the potassium carbonate solution, some side reactions must be considered in the liquid aqueous phase:

$$\mathrm{PZH^+(aq) + H_2O(aq)} \overset{\mathrm{K_{IV}}}{\leftrightarrow} \mathrm{PZ(aq) + H_3O^+(aq)} \quad (R.4)$$

$$PZH_2^{2+}(aq) + H_2O(aq) \overset{K_V}{\leftrightarrow} PZH^+(aq) + H_3O^+(aq) \quad \text{(R.5)}$$

$$PZ(aq) + HCO_3^-(aq) \overset{K_{VI}}{\leftrightarrow} PZCOO^-(aq) + H_2O(aq) \quad \text{(R.6)}$$

$$PZCOO^-(aq) + HCO_3^-(aq) \overset{K_{VII}}{\longleftrightarrow} PZ(COO^-)_2(aq) + H_2O(aq) \quad \text{(R.7)}$$

$$H^+PZCOO^-(aq) + H_2O(aq) \overset{K_{VIII}}{\longleftrightarrow} PZCOO^-(aq) + H_3O^+(aq) \quad \text{(R.8)}$$

where $PZCOO^-$ is piperazine carbamate, $PZ(COO^-)_2$ is piperazine dicarbamate, H^+PZCOO^- is protonated piperazine carbamate, and PZH^+ is protonated piperazine, PZH_2^{2+} is diprotonated piperazine. Reactions (R.1) to (R.8) are water dissociation, bicarbonate formation, carbonate formation, PZ protonation, PZ diprotonation, PZ carbamate formation, PZ dicarbamate formation, and protonated PZ carbamate formation, respectively. The equilibrium constant (K_j) for reactions (R1) to (R8) can be calculated using the temperature-dependent function:

$$\ln K_j = A_1 + \frac{B_1}{T} + C_1 \ln T + D_1 T \quad (21)$$

The parameters of equilibrium constants are summarised in Table 2.

Table 2: Parameters for the chemical equilibrium constant.

Reaction	*A*	*B*	*C*	*D*	Reference
K_I	132.899	-13446	-22.477	0	[37]
K_{III}	216.049	-12432	-35.481	0	[37]
K_{II}	231.465	-12092	-36.781	0	[37]
K_{IV}	241.5	-21918	-34.35	0	[38]
K_V	14.134	2192.3	0	-0.0174	[38]
K_{VI}	-10.15	21980	44.42	0	[31]
K_{VII}	-13.26	1990	0	0	[31]
K_{VIII}	-25.91	-5700	0	0	[31]

2.1.4.2. Kinetic Reactions

Enhancement factors are used to incorporate the effect of slow or kinetically controlled chemical reactions on mass transfer and consequently to account for the liquid side resistance. The enhancement factors are described as the absorption rate ratio with a chemical reaction to the rate without the chemical reaction. Due to the complexity related to enhancement factors determinations, in most studies, analytical expressions are used, which depend on the mass transfer theory and the rate of absorption. The analytical expression of the enhancement factor accounting for the mass transfer describing two films, penetration, and surface renewal theories is a function of a dimensionless number called the Hatta number. The kinetic chemical reactions in the PZ promoted potassium carbonate system are described as follow:

$$CO_2(aq) + OH^-(aq) \rightarrow HCO_3^-(aq) \quad \text{(R.9)}$$

$$HCO_3^-(aq) \rightarrow CO_2(aq) + OH^-(aq) \quad \text{(R.10)}$$

$$PZ(aq) + CO_2(aq) + H_2O(aq) \rightarrow PZCOO^-(aq) + H_3O^+(aq) \quad \text{(R.11)}$$

$$PZCOO^-(aq) + H_3O^+(aq) \rightarrow PZ(aq) + CO_2(aq) + H_2O(aq) \quad \text{(R.12)}$$

$$PZCOO^-(aq) + CO_2(aq) + H_2O(aq) \rightarrow PZ(COO^-)_2(aq) + H_3O^+ \quad \text{(R.13)}$$

$$PZ(COO^-)_2(aq) + H_3O^+(aq) \rightarrow PZCOO^-(aq) + CO_2(aq) + H_2O(aq) \quad \text{(R.14)}$$

The liquid phase mass transfer relations described in Section 2.1.2 must be multiplied by the enhancement factor. The enhancement factor that has been used in this study is as follow [39]:

$$E = Ha = \sqrt{\frac{D_L k}{k_L^2}} \quad (22)$$

where D_L is the diffusivity of CO_2 in piperazine-promoted potassium carbonate solution, k is the overall apparent first-order rate constant ($k_{OH^-}[OH^-] + k_{Amine}[Amine]$), k_L is the liquid side mass transfer coefficient described in equation (20). Details about kinetic reactions are presented by Chen [33] and did not repeat here.

2.1.5. Phase Equilibria Calculations

The phase equilibria calculations (also known as thermodynamic calculations), namely the speciation equilibria (liquid phase equilibria/chemical equilibria); vapour-liquid equilibria (physical equilibria) must also be considered in the model [40].

2.1.5.1. Speciation Calculation (Chemical Equilibrium Calculation)

To estimate the species compositions in the liquid phase composed of CO_2, H_2O, K_2CO_3, and $KHCO_3$, 7 species must be considered: K^+, HCO_3^-, CO_3^{2-}, H^+, OH^-, CO_2, and H_2O. There are 13 unknowns (x_i and γ_i^* for all species except water and γ_w). To find the unknowns, 13 independent equations are required. Five chemical equilibrium constants, three mass balances, one charge balance, nine γ_i^* expressions which must be calculated using a thermodynamic model, and one γ_w expression. In the case of PZ-promoted potassium carbonate solution, 13 species must be considered: K^+, HCO_3^-, CO_3^{2-}, H^+, OH^-, H_2O, CO_2, PZ, $PZCOO^-$, PZH^+, PZH_2^{2+}, H^+PZCOO^-, and $PZ(COO^-)_2$. All the speciation equations for H_2O-K_2CO_3-$KHCO_3$-CO_2 and H_2O-K_2CO_3-$KHCO_3$-PZ-CO_2 systems are:

Total CO_2 Balance For the system without PZ: (23)

$$x_{CO_2} + x_{HCO_3^-} + x_{CO_3^{2-}} = x_{CO_2,Tot}$$

For the system with PZ:

$$x_{CO_2} + x_{HCO_3^-} + x_{CO_3^{2-}} + x_{PZCOO^-} + x_{H^+PZCOO^-} + 2x_{PZ(COO^-)_2} = x_{CO_2,Tot}$$

Total PZ Balance

$$x_{PZ} + x_{PZH_2^{2+}} + x_{PZH^+} + x_{PZCOO^-} + x_{H^+PZCOO^-} + x_{PZ(COO^-)_2} = x_{PZ,Tot} \quad (24)$$

Electro-Neutrality (Charge Balance)

For the system without PZ: (25)

$$x_{H_3O^+} + x_{K^+} = x_{OH^-} + x_{HCO_3^-} + 2x_{CO_3^{2-}}$$

For the system with PZ:

$$x_{H_3O^+} + x_{K^+} + x_{PZH^+} = x_{OH^-} + x_{HCO_3^-} + 2x_{CO_3^{2-}} + 2x_{PZ(COO^-)_2} + x_{PZCOO^-}$$

Chemical Equilibrium Constants

$$K_I = \frac{x_{H_3O^+} \cdot x_{OH^-}}{x_{H_2O}^2} \cdot \frac{\gamma^*_{H_3O^+} \cdot \gamma^*_{OH^-}}{\gamma^2_{H_2O}} \quad (26)$$

$$K_{II} = \frac{x_{H_3O^+} \cdot x_{HCO_3^-}}{x_{CO_2} \cdot x_{H_2O}^2} \cdot \frac{\gamma^*_{H_3O^+} \cdot \gamma^*_{HCO_3^-}}{\gamma^*_{CO_2} \cdot \gamma^2_{H_2O}} \quad (27)$$

$$K_{III} = \frac{x_{H_3O^+} \cdot x_{CO_3^{2-}}}{x_{HCO_3^-} \cdot x_{H_2O}} \cdot \frac{\gamma^*_{H_3O^+} \cdot \gamma^*_{CO_3^{2-}}}{\gamma^*_{HCO_3^-} \cdot \gamma_{H_2O}} \quad (28)$$

$$K_{IV} = \frac{x_{H_3O^+} \cdot x_{PZ}}{x_{PZH^+} \cdot x_{H_2O}} \cdot \frac{\gamma^*_{H_3O^+} \cdot \gamma^*_{PZ}}{\gamma^*_{PZH^+} \cdot \gamma_{H_2O}} \quad (29)$$

$$K_V = \frac{x_{H_3O^+} \cdot x_{PZH^+}}{x_{PZ} \cdot x_{H_2O}} \cdot \frac{\gamma^*_{H_3O^+} \cdot \gamma^*_{PZH^+}}{\gamma^*_{PZ} \cdot \gamma_{H_2O}} \quad (30)$$

$$K_{VI} = \frac{x_{HCO_3^-} \cdot x_{PZ}}{x_{PZCOO^-} \cdot x_{H_2O}} \cdot \frac{\gamma^*_{HCO_3^-} \cdot \gamma^*_{PZ}}{\gamma^*_{PZCOO^-} \cdot \gamma_{H_2O}} \quad (31)$$

$$K_{VII} = \frac{x_{H_3O^+} \cdot x_{PZ(COO^-)_2}}{x_{PZCOO^-} \cdot x_{H_2O}} \cdot \frac{\gamma^*_{H_3O^+} \cdot \gamma^*_{PZ(COO^-)_2}}{\gamma^*_{PZCOO^-} \cdot \gamma_{H_2O}} \quad (32)$$

$$K_{VIII} = \frac{x_{H_3O^+} \cdot x_{PZCOO^-}}{x_{H^+PZCOO^-} \cdot x_{H_2O}} \cdot \frac{\gamma^*_{H_3O^+} \cdot \gamma^*_{PZCOO^-}}{\gamma^*_{H^+PZCOO^-} \cdot \gamma_{H_2O}} \quad (33)$$

Overall mole fraction balance

$$\sum_{i=1}^{n} X_i = 1 \quad (34)$$

where γ_i^* and γ_{H_2O} used in these relations are calculated using the Extended UNIQUAC thermodynamic model. It should be noted that, in this study, the Extended UNIQUAC model

is applied for speciation calculations, vapour-liquid equilibria calculations, and thermal properties estimations in aqueous solutions containing electrolytes and non-electrolyte species.

2.1.5.2. Vapour-Liquid Calculation (Physical Equilibrium Calculation)

CO_2 is the solute, and H_2O is the solvent. In the solution containing CO_2, PZ, and water, for volatile compounds, the vapour-liquid equilibrium relations can be considered as:

$$\mathrm{CO_2(g)} \rightleftharpoons \mathrm{CO_2(aq)} \quad \text{(R.15)}$$

$$\mathrm{H_2O(g)} \rightleftharpoons \mathrm{H_2O(aq)} \quad \text{(R.16)}$$

Table 3 gives Henry's law constant of CO_2 in pure water according to equation (35). The H_e is in Pa, and the temperature is in K. The Henry's constant has been presented by several investigators and has the overall format as:

$$\ln H_e = A_2 + \frac{B_2}{T} + C_2 \ln(T) + D_2 T \quad (35)$$

Table 3: Henry's law constants.

Component	A_2	B_2	C_2	D_2	Reference
CO_2	159.1997	-8477.711	-21.9574	0.00578	[41]

2.1.6. Hydrodynamic Equations

Hydrodynamic relations enable the column outputs to be related to the geometrical aspects and operating conditions; therefore, these relations led to the scale-up design optimisation [42]. Hydrodynamic relations include the liquid hold up, pressure drop, and vapour heat contribution. The liquid holdup is an effective parameter on the packed column operation for calculating the kinetic reaction rates and directly affects the liquid phase mass transfer, loading behaviour, gas-phase pressure gradients, and mass transfer [43]. The particle model hydrodynamic correlations, presented by Stichlmair et al. [44], are used in this study. These correlations are simple and have a greater theoretical consistency than the corresponding channel model hydrodynamic correlations [44]. The hydrodynamic correlations for the liquid holdup, vapour holdup, pressure drop and so on are presented in Table 4.

Table 4: The hydrodynamic correlations for the liquid holdup, vapour holdup, and pressure drop used in this study.

Liquid Volumetric Holdup	$\phi_L = 0.555\left(\frac{V_L^2 \cdot a}{g \cdot \varepsilon^{4.65}}\right)^{1/3}\left(1 + 20\left(\frac{\Delta P_{irr}}{H \cdot \rho_L \cdot g}\right)^2\right)$
Vapor Volumetric Holdup	$\phi_G = \varepsilon - \phi_L$

Dry Bed Pressure Drop	$\frac{\Delta P_{\mathrm{dry}}}{H} = \frac{3 \cdot \mathrm{f_o}}{4}\left(\frac{1-\varepsilon}{\phi^{4.65}}\right)\frac{\rho_G \cdot V_G^2}{\mathrm{d_p}}, \quad \mathrm{f_o} = \frac{\mathrm{C_1}}{\mathrm{Re_G}} + \frac{\mathrm{C_2}}{\sqrt{\mathrm{Re_G}}} + \mathrm{C_3}$ $\mathrm{Re_G} = \frac{\rho_G \cdot V_G \cdot \mathrm{d_p}}{\mu_G}, \quad \mathrm{d_p} = \frac{6 \cdot (1-\varepsilon)}{\mathrm{a}}$
Irrigated Bed Pressure Drop	$\frac{\Delta P_{\mathrm{irr}}}{\Delta P_{\mathrm{dry}}} = \left(\frac{1-\varepsilon+\phi_L}{1-\varepsilon}\right)^{\frac{2+c}{3}}\left(1-\frac{\phi_L}{\varepsilon}\right)^{-4.65}$
Vapor Head Contribution	$\Delta P_{\mathrm{vap}} = H \cdot \rho_L \cdot \phi_G \cdot g$
Overall Pressure Drop	$\Delta P = \Delta P_{\mathrm{irr}} + \Delta P_{\mathrm{vap}}$

where ϕ_L is the liquid volumetric holdup, ϕ_G is the volumetric vapour holdup, ϕ_{Lo} is the pre-loading liquid volumetric holdup, v is the flow velocity, g is gravitational constant, ΔP is the pressure drop over the packed bed, $\Delta \mathrm{P_{vap}}$ is the pressure drop due to the static head of vapour in the packing, H is packing height, ρ is mass density, $\mathrm{f_o}$ is the particle friction factor, Re is the Reynolds number, μ is the viscosity, and $\mathrm{C_1}$, $\mathrm{C_2}$, and $\mathrm{C_3}$ are packing specific constants. The characteristics and required information for packing used in this study are summarised in Table 5.

Table 5: The characteristics of packing for metal random packing used in this study [44].

Packing Type	Type/Size	$\mathbf{d_P}$ (m)	a ($\mathbf{m^2/m^3}$)	$\boldsymbol{\varepsilon}^*$	$\mathbf{C_1}$	$\mathbf{C_2}$	$\mathbf{C_3}$
Flexipac	1Y	0.050	420	0.910	-1.58	0.63	0.84
	AQ style 20	0.060	225	0.930	0.84	-0.11	0.58

*ε is the void fraction, a is surface area of packing and $\mathrm{d_P}$ is the packing diameter.

2.1.7. Thermodynamic Models and Physical Properties

To accurately determine the non-ideal behaviour of the potassium carbonate process, special properties and thermodynamic models are required. In rate-based modelling and simulation, the absorption processes detail speciation of all species in the liquid phase, including ions, and appropriate acidity coefficients are required [45]. Various property calculations methods and models can be achieved from literature or empirical correlations [46]. Thermodynamic and physical property models used in this study are summarised by their references in Table 6.

Table 6: Thermodynamic and physical property models are used in the rate-based model of the PZ-promoted potassium carbonate process.

Phase	Property	Model Name	Reference
	Mixture molar enthalpy	Extended UNIQUAC	[47]
	Mixture molecular weight	Weighted Average	[46]
	Activity coefficients	Extended UNIQUAC	[47]
	Diffusivity of a component in a mixture	Wilke-Chang modification	[46]

Liquid	Mixture molar volume	Brelvi-O'Connell	[37]
	Mixture viscosity	Empirical Correlation	[48]
	Mixture molar density	Empirical Correlation	[48]
	Mixture heat capacity	Empirical Correlation	[48]
	Mixture thermal conductivity	Empirical Correlation	[49]
	Mixture surface tension	Empirical Correlation	[49]
	Vapour Pressure	Extended Antoine	[49]
Gas	Mixture molar enthalpy	Soave-Redlich-Kwong	[46]
	Mixture molecular weight	Weighted Average	[46]
	Fugacity coefficients	Soave-Redlich-Kwong	[46]
	Diffusivity of a component in a mixture	Blanc's law	[46]
	Mixture molar volume	Soave-Redlich-Kwong	[46]
	Mixture viscosity	Chung *et al.* (1988) Rule	[50]
	Mixture molar density	Soave-Redlich-Kwong	[46]
	Mixture heat capacity	Empirical Correlation	[46]
	Mixture thermal conductivity	Chung *et al*. (1988) method	[50]

The Extended UNIQUAC thermodynamic model [51] and the property models were applied to complete the physical and thermodynamic calculations for the non-equilibrium rate-based modelling of the piperazine-promoted potassium carbonate process. Extended UNIQUAC includes volume and surface area parameters and energy interaction parameters. Many experimental data were collected and used to obtain the optimum interaction parameters using regression for the Extended UNIQUAC model for PZ-promoted potassium carbonate solution. The used experimental data [52–62] are illustrated in Table S.1. However, some of the parameters are extracted from literature [47]. The parameters of Extended UNIQUAC are summarized in Tables S.2-S.4.

2.2. Model Solution

In the absorber column of potassium carbonate, the gas stream is fed at the bottom. The lean PZ-promoted potassium carbonate solution is fed at the top of the column. These two streams are specified completely. The treated gas and rich solution, which leave the absorber's top and bottom, respectively, usually are incompletely specified. Thus, the state of non-ends of the column is not specified fully, which leads to a two-point boundary value problem. The diversity of problems of the boundary value type has generated a variety of methods for their solution, methods such as the shooting method, the finite difference method, and the collocation method. In this work, the collocation method is used. The collocation method is available in MATLAB software under the name *bvp4c* and *bvp5c*, which is used to solve the model's equations.

2.3. Model Validation and Results Analysis

There are pilot plant scale data on the CO_2 absorption by PZ promoted potassium carbonate solutions [33]. This data is used to validate the results obtained from the model. To analysis the model, various charts and profiles are plotted.

3. Results and Discussion

3.1. Thermodynamic modelling results

The predicted CO_2 partial pressures and experimental data for in 20 wt% equivalent concentration of potassium carbonate solution (with the solution containing CO_2, H_2O, K_2CO_3, and $KHCO_3$) and for a solution including 5 m of potassium ion and 2.5 m piperazine (the solution containing CO_2, H_2O, PZ, K_2CO_3, and $KHCO_3$) are compared in Figure 2 and Figure 3 respectively. In general, there is a good agreement between the model predictions and the experimental values. As can be seen in Figure 2 and Figure 3 the isotherms predicted by the Extended UNIQUAC thermodynamic model are nearly parallel. This is possibly caused by the constant enthalpy (heat) of absorption with changes in loading. The amount of loading has a considerable effect on the calculations since for the loadings lower than one, the CO_2 is significantly converted to bicarbonate and the amount of free CO_2 in the solution is negligible [59]. In this work, the Extended UNIQUAC model predicted the CO_2 solubility data of Tosh et al. [63] in 20% equivalent concentration of K_2CO_3 with average absolute relative deviation (AARD%) around 10.9% which is comparable with the works of Cullinane [64] and Hilliard [59]. In addition, the model predicted the CO_2 solubility data of Hilliard [59] for 2.5 m PZ plus 5 m potassium ion with an average absolute relative deviation of around 13.52%.

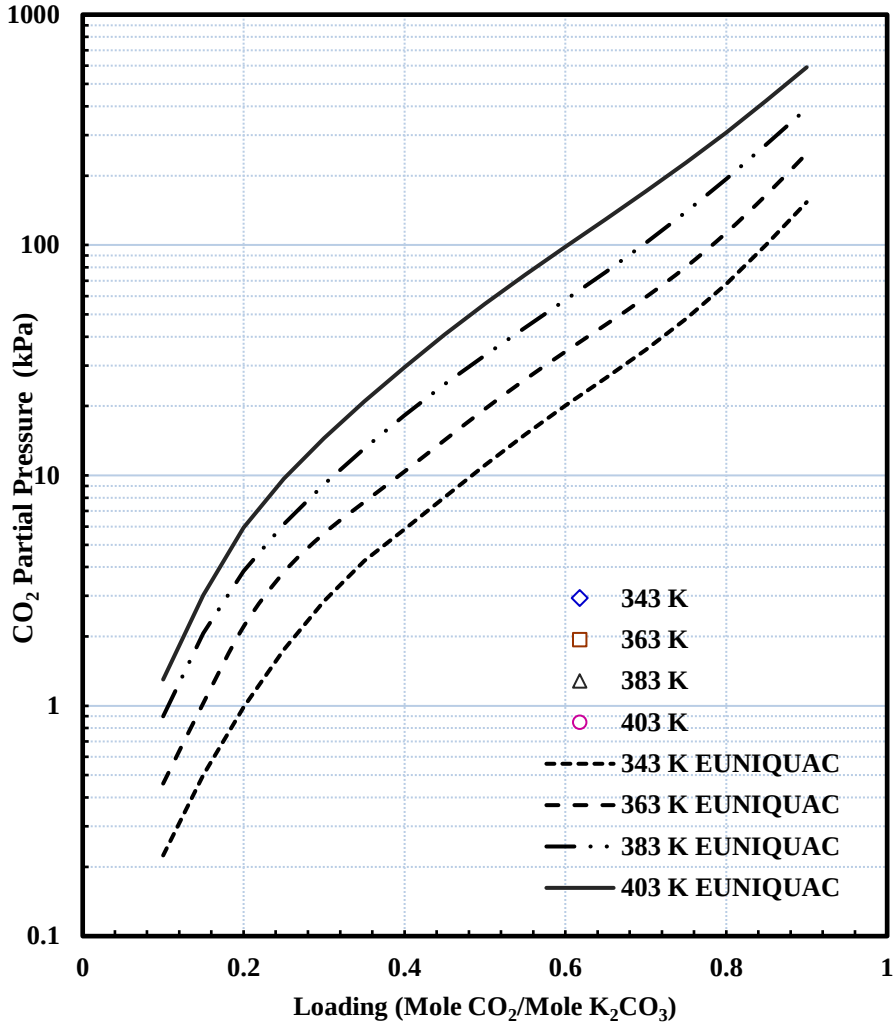

Figure 2: CO_2 partial pressure in 20 wt% equivalent concentration of potassium carbonate solution at four different temperatures; Points: [63]; Lines: Extended UNIQUAC.

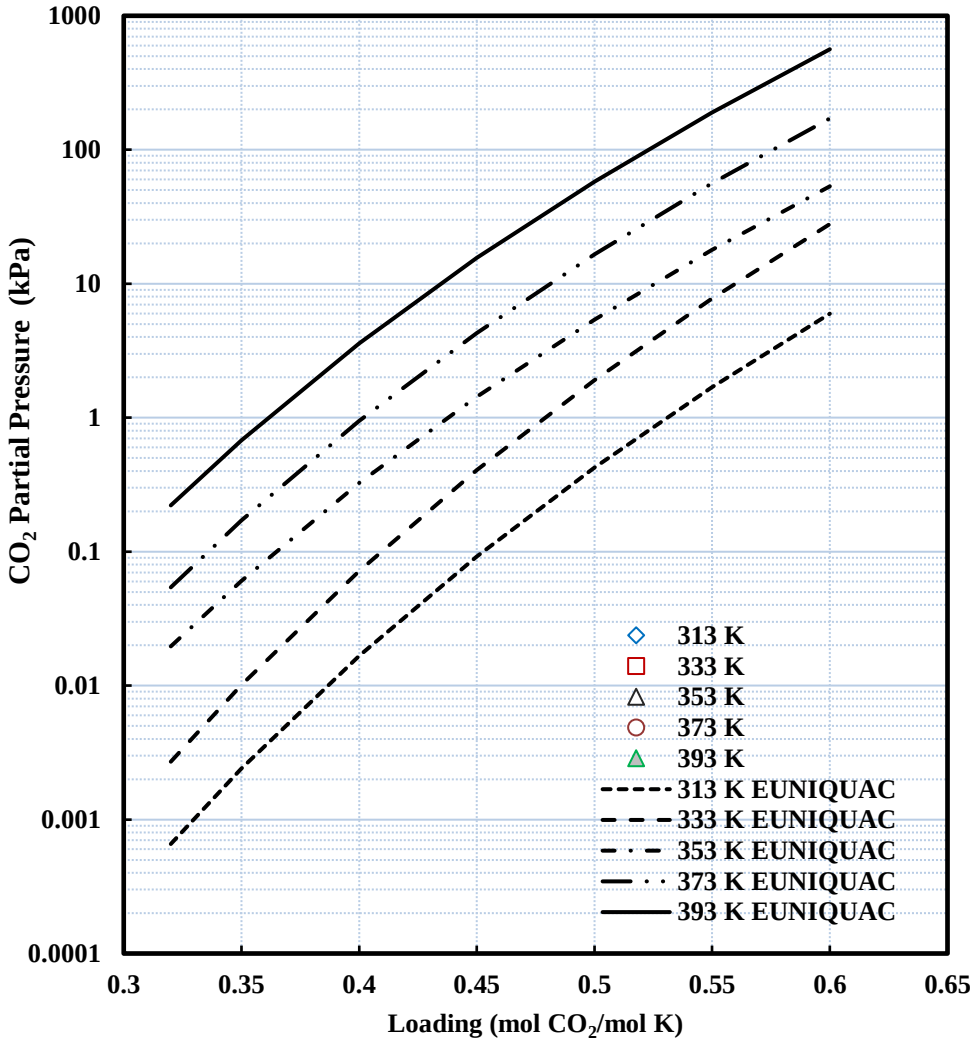

Figure 3: CO_2 partial pressure in the solution contains 5 m of potassium ion plus 2.5 m piperazine at five different temperatures; Points: [59] and [62]; Lines: Extended UNIQUAC.

3.2. Process modelling results

In this study, the PZ-promoted potassium carbonate process pilot plant data presented by Chen [33] are used to validate the developed model. Chen [33] developed a rate-based model for his experimental data. However, he mainly focused on the effective interfacial area and average heat losses. The author [33] also optimised the absorber column with respect to its height and diameter and a comprehensive sensitivity analysis has been carried out. It has been highlighted that understanding solvent composition is essential for the study of CO_2 removal for PZ promoted potassium carbonate process. Chen et al. [33] have carried out a multitude of pilot plant experiments, with data available for three experimental set up, with the first two using a absorbent compositions of 5 m K^+ + 2.5 m PZ with two types of packing namely Flexipac 1Y and Flexipac AQ 20, and the third using a composition of 6.4 m K^+ + 1.6 m PZ and Flexipac

AQ 20 as packing. Concentrations of PZ and K_2CO_3 were measured using titration and chromatography methods, with a precision of approximately ±10%. In all columns, a chimney tray and liquid redistributors were used between each bed of packing. The gas stream contains CO_2, which enter the absorber column is a synthetic gas contained CO_2, N_2, and water. The process flow diagram of the absorption-desorption pilot plant is illustrated in Figure 4.

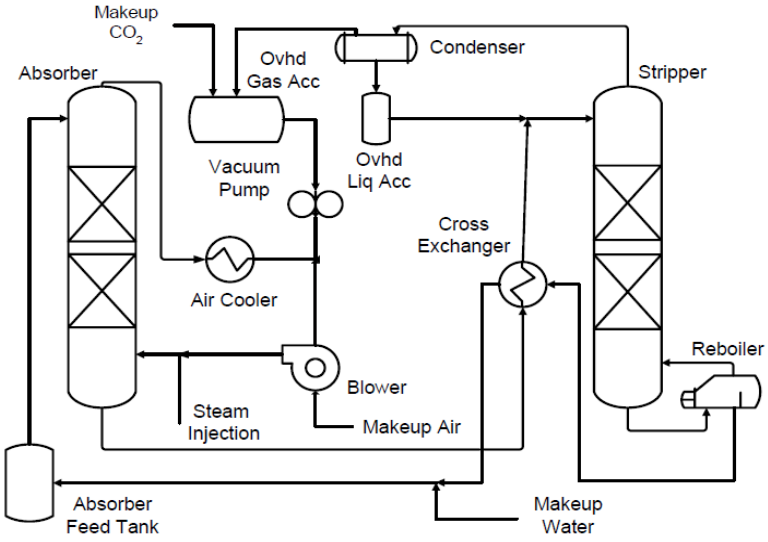

Figure 4: Schematic diagram of absorber and stripper of PZ-K_2CO_3 process [33].

The characteristics of the absorber column reported by Chen [33] are demonstrated in Table 7. It should be noted that in the data presented by Chen [33], the profiles for the CO_2 mole fraction in the gas phase, CO_2 loading, and temperature along the column were not report. Therefore, no data exists for the mentioned properties along the column. However, other studies on chemical reactive absorption processes can be inferred from to understand the profile of the missing information along the column. For example, the study of Tontiwachwuthikul et al. [65] has been used in a considerable number of studies [66,67]. The component concentration can be converted to the mole fractions using the following relations:

$$n_{K_2CO_3} = m_{K^+}/2 \quad (36)$$

$$n_{\mathrm{PZ}} = m_{\mathrm{PZ}} \quad (37)$$

$$n_{CO_2^{tot}} = m_{CO_2^{tot}} = \mathrm{Ldg}.\,(2n_{\mathrm{PZ}} + n_{K^+}) \quad (38)$$

$$n_{\mathrm{H_2O}} = 1000/Mw_{\mathrm{H_2O}} = 55.508 \quad (39)$$

$$x_i = n_i/\sum n_i \quad (40)$$

wherein these relations m_{i} is the molality of component i (mol/kg H_2O), x_i is the mole fraction of component i ($\sum x_i = 1$), n_i is the number of moles of component i, Ldg is the CO_2 loading of solution (mol $\mathrm{CO_2^{tot}}$/mol $\mathrm{K^+}$ + 2mol PZ), and Mw_i is the molecular weight of component *i* (gr/mol).

In this study, 10 stages are considered for the absorber column model given that using this number of stages, an agreement is observed between the model and experimental data in terms of the CO_2 concentration in the outlet gas stream and adding more stages did not resulted in considerable separation. Experimental data reported by Chen [33] is used to validate the model in this study. The composition of the solvent blend is 5 m K^+ + 2.5 m PZ solution and 6.4 m K^+ + 1.6 m PZ using two different types of packing. Three different experimental runs have been selected to validate the process model. More details about the experimental data that have been used in this study can be found in Table 7.

Table 7: Characteristics of the absorber of PZ-K_2CO_3 process [33].

Run	**1**	**2**	**3**
Solvent Composition	5 m K^+ +2.5 m PZ	5 m K^+ +2.5 m PZ	6.4 m K^+ +1.6 m PZ
Column Diameter (m)	0.427	0.427	0.427
Column Height (m)	10.7	10.7	10.7
Packing Height (m)	6.1	6.1	6.1
Packing Type	Flexipac 1Y	Flexipac AQ 20	Flexipac AQ 20
Absorber Pressure (bar)	1	1	1
K_2CO_3 concentration (mol/kg solvent) in the solution	1.5	1.5-2	1.8-2.4
PZ concentration (mol/kg solvent) in the solution	1.3-1.4	1.4-1.5	1.0-1.2
K^+/PZ mole ratio	2.0-2.3	2.1-2.3	3.9-4.0
Inlet CO_2 (mol%)	2.6-12.6	8.0-17.6	14.3-18.0
Gas Rate (kg/m^2.s)	1.2-2.2	1.2-2.0	1.2-2.0
L/G (kg/kg)	1.7-7.1	3.9-10.8	8.3-14.5
Inlet Gas Temperature (℃)	30-64	40	40-41
Lean Liquid Temperature (℃)	39-48	40-46	39-46
Lean CO_2 Loading (mol CO_2/(mol K^++2 mol PZ))	0.43-0.54	0.39-0.45	0.45-0.51

The rate-based model characteristics and the modelling results according to the selected pilot plant runs are presented in Table 8. In this table, the experimental temperatures of inlet and outlet gas and liquid streams are listed according to Chen [33]. The predicted temperatures are compared to the experimental amounts. As can be seen, the predicted amounts of outlet gas stream are higher than experimental amounts considerably, which maybe due to the high amount of heat of CO_2 absorption in the solution and some heat loss amounts in the pilot plant data. For the liquid stream, the temperatures show more match the experimental data.

Table 8: Summary of rate-based model predictions and selected experimental data.

Run	**1**				**2**				**3**			
Number	**1.1**	**1.2**	**1.3**	**1.4**	**2.1**	**2.2**	**2.3**	**2.4**	**3.1**	**3.2**	**3.3**	**3.4**
Exp. Inlet gas stream temperature (℃)	47.2	50.8	47.2	47.1	40.1	40.1	39.9	40.5	41.1	38.7	40	40
Exp. Inlet liquid stream temperature (℃)	41.2	41.4	41.2	40.1	46.7	45.0	43.3	40.0	38.8	39.5	40	39.4
Exp. Outlet gas stream temperature (℃)	38.6	45.8	38.6	36.3	46.7	43.4	47.2	37.3	34.1	36.8	36.6	35.3
Calc. Outlet gas stream temperature (℃)	42.8	51.8	47.0	44.5	50.6	56.4	54.3	53.3	45.6	47.0	40.8	42.2
Exp. Outlet liquid stream temperature (℃)	45.9	46.6	48.0	48.0	50.9	50.6	47.3	51.2	43.7	44.5	46.2	46.1
Calc. Outlet liquid stream temperature (℃)	49.4	46.8	51.6	53.7	54.6	53.8	50.6	55.1	49.8	52.2	52.8	53.6
Absorber operation pressure (atm)	1	1	1	1	1	1	1	1	1	1	1	1
Gas stream flow (m^3/min)	12.7	17.0	9.9	14.2	8.5	11.3	14.2	14.2	8.5	8.5	8.5	8.5
Exp. CO_2 in inlet gas stream	0.104	0.117	0.119	0.162	0.1663	0.1277	0.1075	0.1394	0.1572	0.1664	0.1669	0.1517
Exp. H_2O in inlet gas stream	0.07	0.07	0.07	0.07	0.07	0.07	0.07	0.07	0.07	0.07	0.07	0.07
Exp. N_2 in inlet gas stream	0.826	0.813	0.811	0.768	0.763	0.802	0.822	0.790	0.7728	0.763	0.763	0.778
Liquid stream flow (L/min)	47.2	49.4	43.7	77.4	45.4	54.8	55.1	75.8	87.0	79.3	68.2	56.8
Exp. Density liquid out (kg/ m^3)	1237.0	1238.0	1238.0	1233.0	1230.0	1228.0	1227.0	1223.0	1275	1265.0	1266.0	1267.0
Calc. Density liquid out (kg/ m^3)	1240.4	1244.6	1239.8	1236.1	1235.9	1236.5	1239.7	1233.6		1288.5	1288.3	1287.2
Exp. CO_2 in outlet gas stream	0.019	0.040	0.019	0.020	0.023	0.010	0.019	0.019	0.049	0.036	0.052	0.043
Calc. CO_2 in outlet gas stream	0.018	0.044	0.017	0.032	0.024	0.013	0.016	0.014	0.048	0.037	0.053	0.042

As can be seen in Table 8, the rate-based model can predict the CO_2 mole fraction in the outlet gas stream in quantitative agreement with experimental data. Other properties are also accurately predicted.

Figure 5 shows the CO_2 concentration profile for the gas phase in the PZ promoted potassium carbonate process using the Bravo and Fair [36] mass transfer correlation. For all cases, most of the CO_2 is removed from the gas stream at the top of the column (stage 1) given that at the top, the liquid solution is CO_2 lean, leading to the highest-pressure gradient, and mass transfer of CO_2 from the gas to the liquid phase. According to Table 7, the differences between Run 1.1 and 2.1 is related to the type of packing (Flexipac 1Y vs Flexipac AQ 20) and mole fraction of CO_2 in the inlet gas stream with the same composition of solvent (5 m K^+ +2.5 m PZ). Run 1.1 and 2.1 showing the same trend. The CO_2 concentration in the inlet gas stream for Run 2.1 and 3.1 is almost the same. As can be seen the CO_2 concentration for Run 2.1 decreasing more dramatically than Run 3.1 and the final value of the CO_2 in the outlet gas stream for Run 3.1 is more than the value of CO_2 in the outlet gas stream for Run 2.1. This showing that more amount of PZ (2.5 m vs 1.6 m) can result in more separation of CO_2.

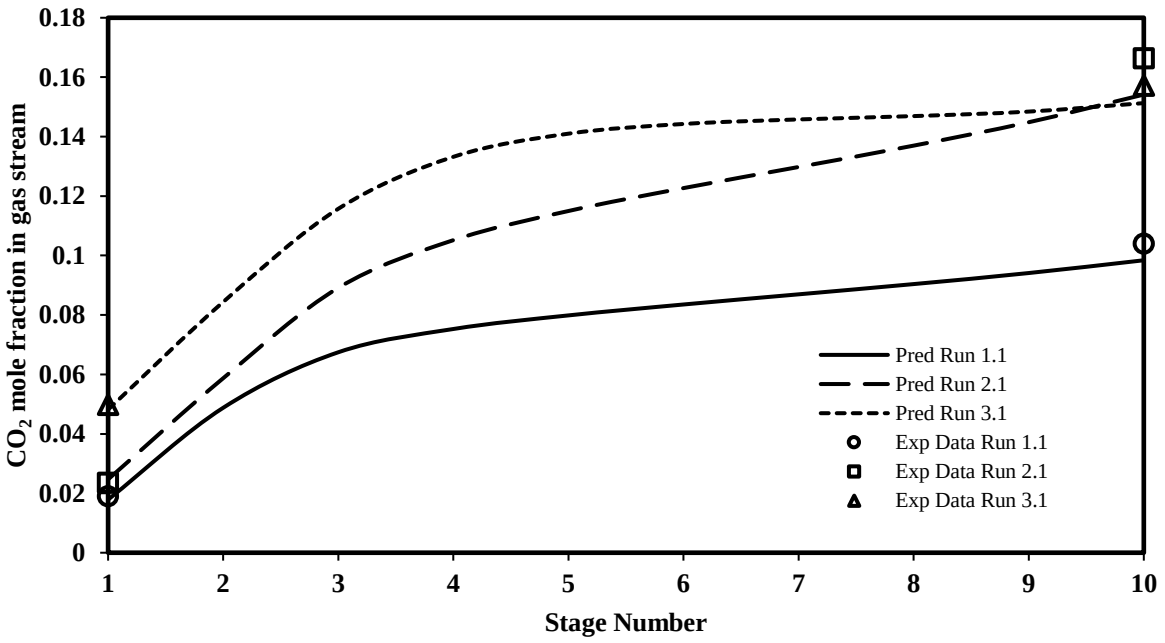

Figure 5: CO_2 mole fraction profile in the gas stream along the packed column.

The liquid temperature profile for three selected runs is presented in Figure 6. The temperature reaches a maximum at intermediate stages. This maximum is important in the liquid phase as it significantly affects the absorption rates in the column since the kinetics of the absorption reaction, the phase equilibrium of the system, and all fluid transport properties depend on the temperature. The existence of the maximum can be explained based on the balance of the heat

released from the reaction of CO_2 with the liquid solution and the heat consumed by processes including water evaporation, heating of the liquid and gas streams, and heat loss to the environment. If the heat released from the absorption reaction is more than the heat consumed, the temperature will rise. According to the shape of the temperature maximum (bulge), Zhang *et al*. [68] considered three absorber temperature profiles.

The shapes of the temperature profiles for gas and liquid phases are similar, and the difference in the temperature of the phases is related to the differences in their heat capacities [69]. Interestingly, As can be seen in Figure 6, given that the first two experimental runs (run 1.1 and run 1.2) are using the same solvent concentrations (2.5 m K^+ + 2.5 m PZ), the temperature profiles are similar with a broad maximum region. The temperature profile of run 3.1 is slightly different given the different solvent composition (6.4 m K^+ + 1.6 m PZ solution) having a narrower peak. However, in general, all three runs show a maximum near the top of the column. This is different to the maxima observed in DEA-promoted potassium carbonate solutions and other chemical solvents [70], which is maybe related to the high heat of absorption of CO_2 in the PZ-promoted potassium carbonate solution, leading to a sudden increase in temperature near the gas inlet.

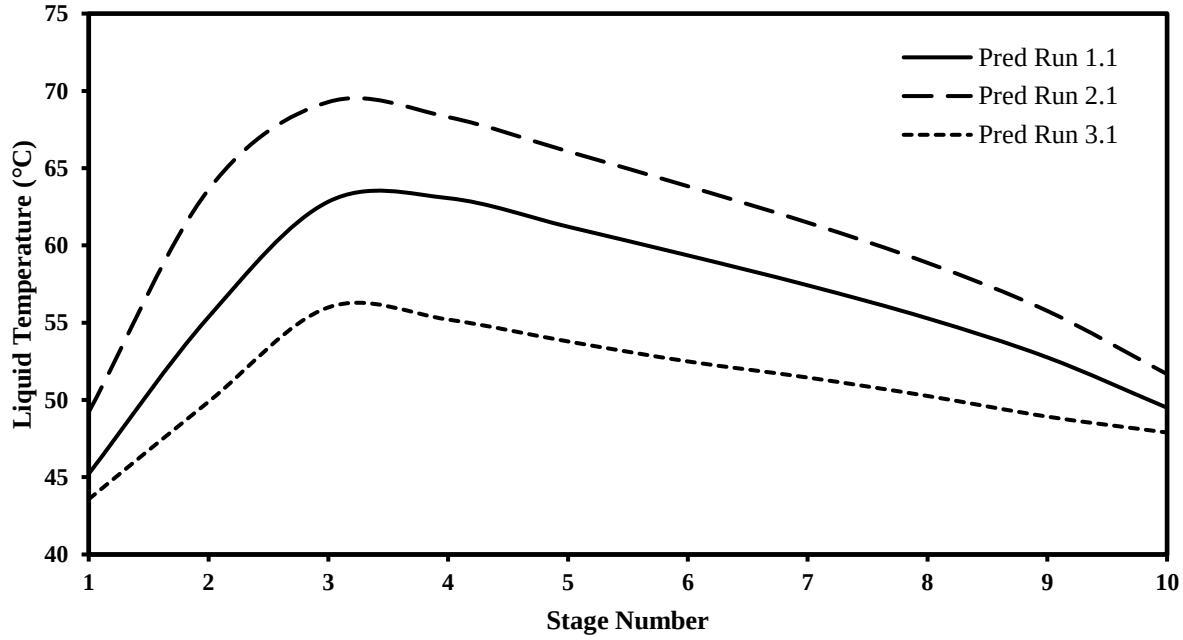

Figure 6: Temperature profile of the liquid stream against stage number.

Liquid and gas flow rate profiles along the packed column are presented in Figure 7 and Figure 8, respectively. Flowrates are generally highest near the top of the column and decrease with the number of stages. By flowing the gas to the top of the column and moving the liquid stream to the bottom of the column, the flow rates decrease.

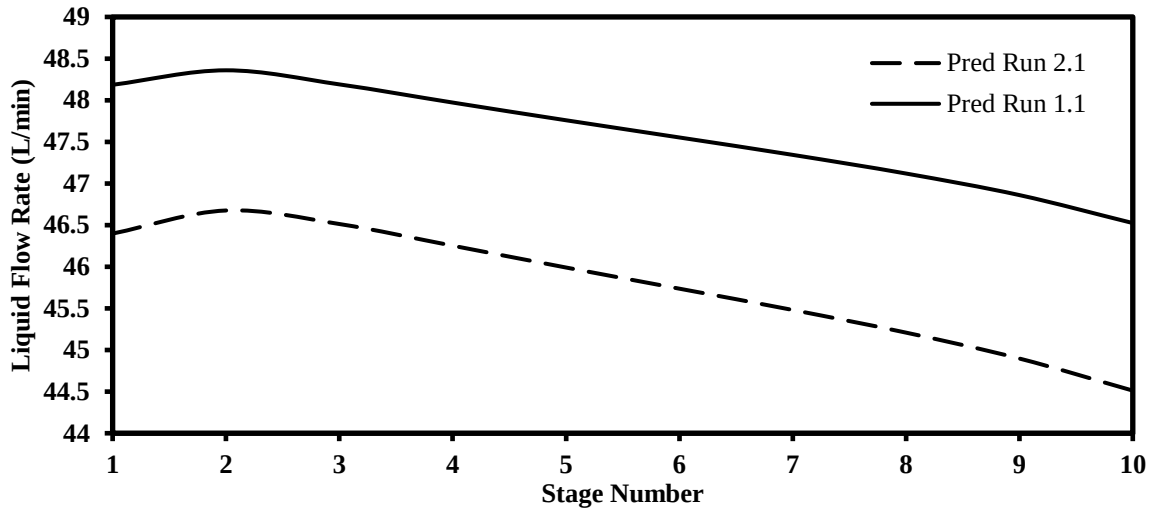

Figure 7: Liquid flow rate profile along the packed column.

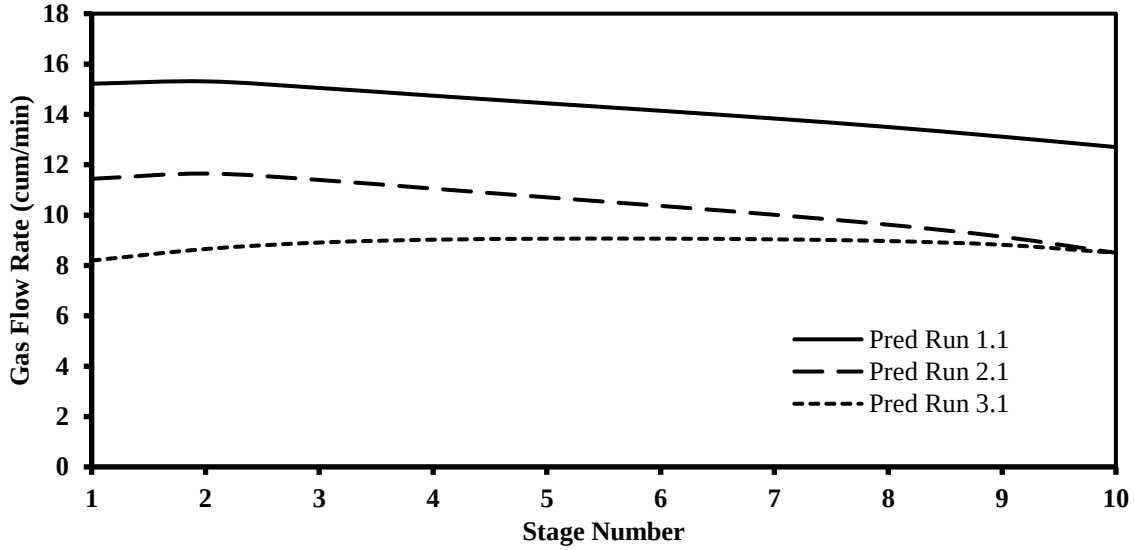

Figure 8: Gas flow rate profile along the packed column.

Figure 9 shows the CO_2 loading profile for the three selected runs. The loading here is defined by the moles of CO_2 divided by the moles of K^+ ion added to two times the number of moles of PZ (mol CO_2/mol K^++ 2 mol PZ). In all the curves, liquid loading is low in the first stage. By increasing the stages, the loading increases dramatically, which is related to the liquid solution's saturation. The loading at the bottom of the column does not show any considerable change. These are in agreement with the results of Tontiwachwuthikul *et al*. [65] and Afkhamipour and Mofarahi [35].

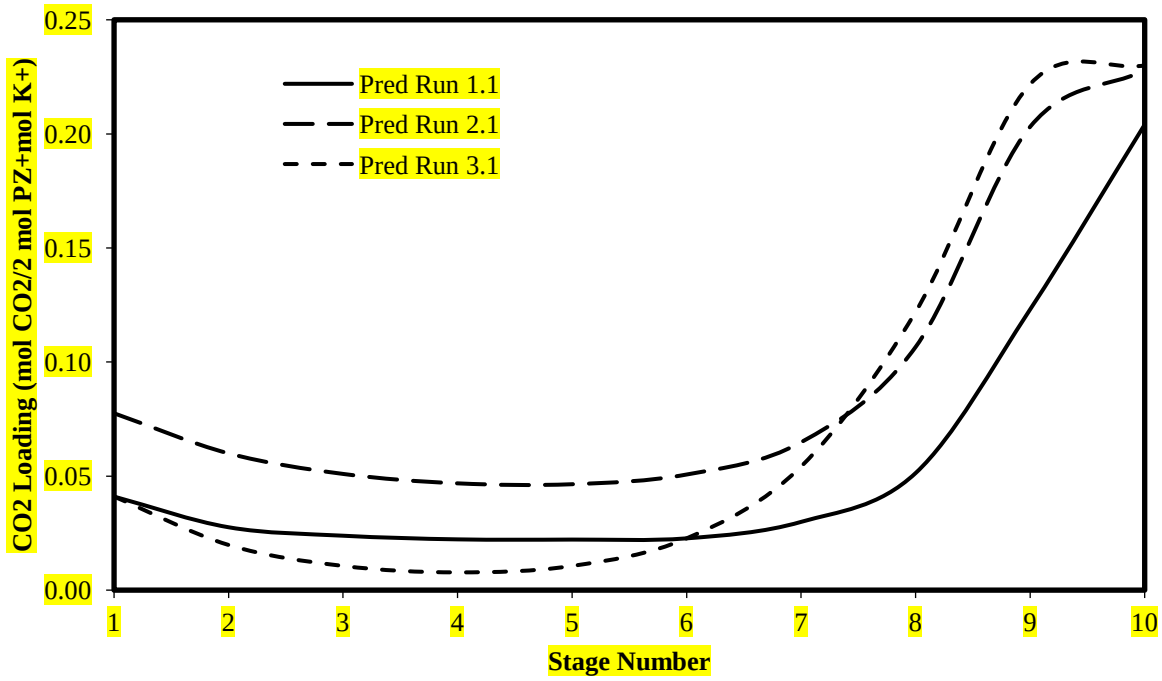

Figure 9: Profile of CO_2 loading along the packed column.

Figure 10 presents the profile of mole fraction of H_2O in the gas phase. At the bottom of the column (stage 10), some water evaporates from the liquid solution since the high-temperature of the gas stream increases the system temperature so that the water vapour pressure increases, leading to a higher water vapour content. Also, the heat released due to the absorption of CO_2 can increase water vapour content, with its contribution being very significant near the top of the column for runs 1.1 and 2.1, where most of the CO_2 is absorbed into the liquid. Interestingly, for run 3.1, the water vapour content slightly decreases going from the bottom of the column to the top.

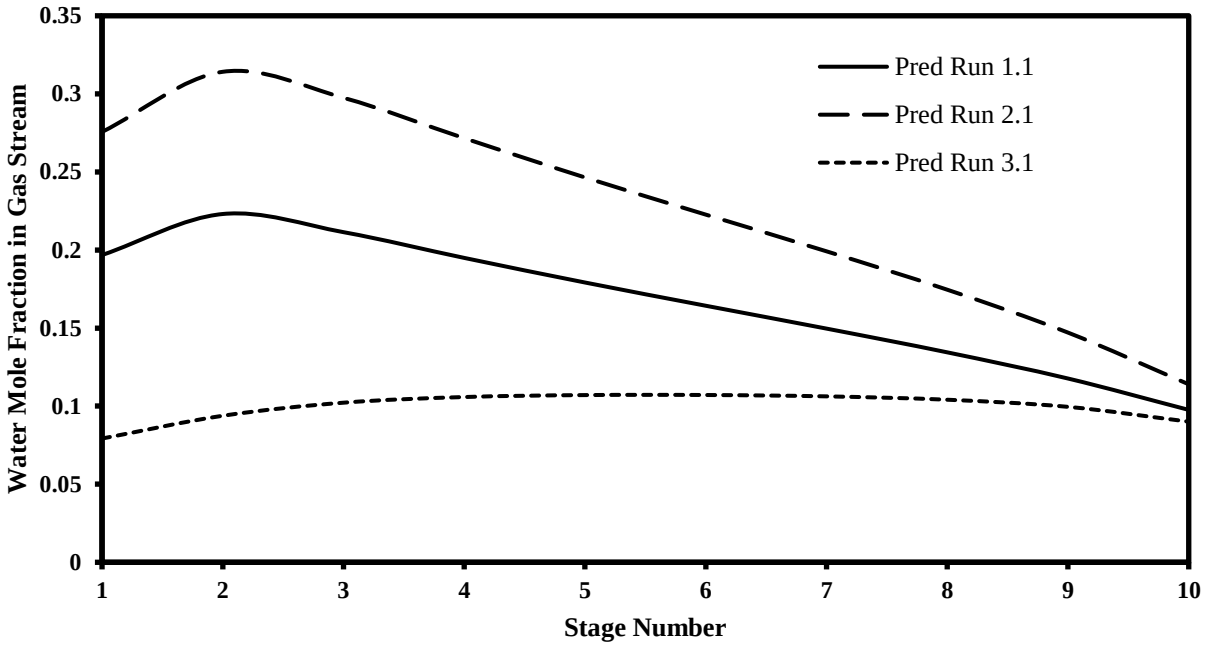

Figure 10: H_2O mole fraction profile in the gas stream along the packed column.

4. Conclusions

A rate-based non-equilibrium model has been constructed for piperazine promoted potassium carbonate solution in MATLAB software. A pilot plant experimental data for the piperazine-promoted potassium carbonate process have been used to construct and validate the model. The focus has been proposed to the CO_2 removal amount in comparison with the experimental data from literature. The results show a good agreement between the predicted and experimental data. CO_2 concentration profiles along the column show a reasonable trend, which has been validated against experimental data, where information about inlet and outlet compositions and temperatures are provided. The liquid temperature profile for three selected runs has been illustrated. The profile shows a maximum at intermediate stages near the top of the column, different to other typical amine solutions. Profiles of liquid and gas flow rates are also presented against the stage number. The flow rates decrease by moving the gas flow to the top of the column and moving the liquid stream to the bottom of the column. Besides, the CO_2 loading profile for three columns has been proposed along the column. However, there was no experimental data for these profiles, yet the trend is in qualitative agreement with other studies on reactive chemical absorptions of CO_2. The profile of H_2O amount in the gas phase suggests the presence of water vapour throughout the column, meaning that in the bottom of the column, some amounts of water evaporate from the liquid solution. In addition, this study provides a framework to model a complex mixture for CO_2 absorption.

Nomenclature

a_p	Total surface area of packing (m^2/m^3)
a_w	Wetted surface area of packing (m^2/m^3)
D_L	Diffusivity of CO_2 in (m^2/s)
f_o	particle friction factor (-)
g	Gravitational constant (m/s^2)
H	Packing height (m)
H_e	Henry's constant of component ($kPa.m^3/kmol$)
K_{G_i}	Overall gas phase mass transfer coefficient of component i ($kmol/(m^2.kPa.s)$)
k_L	Mass transfer coefficient in liquid phase (m/s)
Ldg	CO_2 loading of solution ($mol\ CO_2^{tot}/mol\ K^+ + 2mol\ PZ$)
m	Molal (mol/kg H_2O)
m_i	molality of component i (mol/kg H_2O)
Mw_i	molecular weight of component i (gr/mol)
N_i	Absorption rate of component i into potassium carbonate solution (-)
P_i	Partial pressure of component i (kPa)
P_i^*	Equilibrium partial pressure of component i (kPa)
Re	Reynolds number (-)
T_g	Gas phase temperature (K)
T_l	Liquid phase temperature (K)
v	Velocity (m/s)
x_i	mole fraction of component i (-)
n_i	number of moles of component i (-)

Greek Symbols

ϕ_G	Vapour volumetric holdup (-)
ϕ_L	liquid volumetric holdup (-)
ϕ_o	Pre-loading liquid volumetric holdup (-)
ρ	Density (kg/m^3)
μ	Viscosity (m^2/s)
ΔP	Pressure drop over the packed bed (kPa)
ΔP_{vap}	Pressure drop due to the static head of vapour in the packing (kPa)

Abbreviations

AMP	2-Amino-2-methyl-1-propanol
BZA	Benzylamine
DEA	Diethanolamine
DIPA	Diisopropanolamine
MEA	Monoethanolamine
MDEA	N-methyldiethanolamine
PZ	Piperazine

References

[1] Zhang Z, Borhani TN, Olabi AG. Status and perspective of CO2 absorption process. Energy 2020;205:118057. https://doi.org/https://doi.org/10.1016/j.energy.2020.118057.

[2] N.Borhani T, Wang M. Role of solvents in CO2 capture processes: The review of selection and design methods. Renew Sustain Energy Rev 2019;114.

https://doi.org/10.1016/j.rser.2019.109299.

[3] Borhani TN, Wang M. Role of solvents in CO2 capture processes: the review of selection and design methods. Renew Sustain Energy Rev 2019.

[4] Shi H, Huang M, Huang Y, Cui M, Idem R. CO2 absorption efficiency of various MEA-DEA blend with aid of CaCO3 and MgCO3 in a batch and semi-batch processes. Sep Purif Technol 2019;220:102–13. https://doi.org/https://doi.org/10.1016/j.seppur.2019.03.048.

[5] Borhani TN, Oko E, Wang M. Process modelling and analysis of intensified CO2 capture using monoethanolamine (MEA) in rotating packed bed absorber. J Clean Prod 2018;204:1124–42. https://doi.org/10.1016/j.jclepro.2018.09.089.

[6] Borhani TNG, Afkhamipour M, Azarpour A, Akbari V, Emadi SH, Manan ZA. Modeling study on CO<inf>2</inf>and H<inf>2</inf>S simultaneous removal using MDEA solution. J Ind Eng Chem 2016. https://doi.org/10.1016/j.jiec.2015.12.003.

[7] Ghiasi MM, Hajinezhad A, Yousefi H, Mohammadi AH. CO2 loading capacity of DEA aqueous solutions: Modeling and assessment of experimental data. Int J Greenh Gas Control 2017;56:289–301. https://doi.org/https://doi.org/10.1016/j.ijggc.2016.11.029.

[8] Rochelle G, Chen E, Freeman S, Van Wagener D, Xu Q, Voice A. Aqueous piperazine as the new standard for CO2 capture technology. Chem Eng J 2011;171:725–33. https://doi.org/https://doi.org/10.1016/j.cej.2011.02.011.

[9] van der Ham L V, Romano MC, Kvamsdal HM, Bonalumi D, van Os P, Goetheer EL V. Concentrated Aqueous Piperazine as CO2 Capture Solvent: Detailed Evaluation of the Integration with a Power Plant. Energy Procedia 2014;63:1218–22. https://doi.org/https://doi.org/10.1016/j.egypro.2014.11.131.

[10] Shokouhi M, Zoghi AT, Vahidi M, Moshtari B. Solubility of Carbon Dioxide in Aqueous Blends of 2-Amino-2-methyl-1-propanol and N-Methyldiethanolamine. J Chem Eng Data 2015;60:1250–8. https://doi.org/10.1021/je500860v.

[11] Cuccia L, Dugay J, Bontemps D, Louis-Louisy M, Morand T, Kanniche M, et al. Monitoring of the blend monoethanolamine/methyldiethanolamine/water for post-combustion CO2 capture. Int J Greenh Gas Control 2019;80:43–53. https://doi.org/https://doi.org/10.1016/j.ijggc.2018.11.004.

[12] Closmann F, Nguyen T, Rochelle GT. MDEA/Piperazine as a solvent for CO2 capture. Energy Procedia 2009;1:1351–7. https://doi.org/https://doi.org/10.1016/j.egypro.2009.01.177.

[13] Costa C, Demartini M, Di Felice R, Oliva M, Pagliai P. Piperazine and methyldiethanolamine interrelationships in CO2 absorption by aqueous amine mixtures. Part I: Saturation rates of single-reagent solutions. Can J Chem Eng 2019;97:1160–71.

[14] Zhan J, Wang B, Zhang L, Sun B-C, Fu J, Chu G, et al. Simultaneous Absorption of H2S and CO2 into the MDEA+ PZ Aqueous Solution in a Rotating Packed Bed. Ind Eng Chem Res 2020;59:8295–303.

[15] Choi W-J, Cho K-C, Lee S-S, Shim J-G, Hwang H-R, Park S-W, et al. Removal of carbon dioxide by absorption into blended amines: kinetics of absorption into aqueous AMP/HMDA{,} AMP/MDEA{,} and AMP/piperazine solutions. Green Chem 2007;9:594–8. https://doi.org/10.1039/B614101C.

[16] Kvamsdal HM, Ehlers S, Kather A, Khakharia P, Nienoord M, Fosbøl PL. Optimizing integrated reference cases in the OCTAVIUS project. Int J Greenh Gas Control 2016;50:23–36. https://doi.org/https://doi.org/10.1016/j.ijggc.2016.04.012.

[17] Afkhamipour M, Mofarahi M, Rezaei A, Mahmoodi R, Lee C-H. Experimental and theoretical investigation of equilibrium absorption performance of CO2 using a mixed 1-dimethylamino-2-propanol (1DMA2P) and monoethanolamine (MEA) solution. Fuel 2019;256:115877. https://doi.org/https://doi.org/10.1016/j.fuel.2019.115877.

[18] Conway W, Beyad Y, Richner G, Puxty G, Feron P. Rapid CO2 absorption into aqueous benzylamine (BZA) solutions and its formulations with monoethanolamine (MEA), and 2-amino-2-methyl-1-propanol (AMP) as components for post combustion capture processes. Chem Eng J 2015;264:954–61. https://doi.org/https://doi.org/10.1016/j.cej.2014.11.040.

[19] Gao H, Liu S, Gao G, Luo X, Liang Z. Hybrid behavior and mass transfer performance for absorption of CO2 into aqueous DEEA/PZ solutions in a hollow fiber membrane contactor. Sep Purif Technol 2018;201:291–300. https://doi.org/https://doi.org/10.1016/j.seppur.2018.03.027.

[20] Sutar PN, Vaidya PD, Kenig EY. Activated DEEA solutions for CO2 capture—A study of equilibrium and kinetic characteristics. Chem Eng Sci 2013;100:234–41. https://doi.org/https://doi.org/10.1016/j.ces.2012.11.038.

[21] Nwaoha C, Tontiwachwuthikul P, Benamor A. CO2 capture from lime kiln using AMP-DA2MP amine solvent blend: A pilot plant study. J Environ Chem Eng 2018;6:7102–10. https://doi.org/https://doi.org/10.1016/j.jece.2018.11.007.

[22] Hamidi R, Farsi M, Eslamloueyan R. CO2 solubility in aqueous mixture of MEA,

MDEA and DAMP: Absorption capacity, rate and regeneration. J Mol Liq 2018;265:711–6. https://doi.org/https://doi.org/10.1016/j.molliq.2018.07.013.

[23] Borhani TNG, Azarpour A, Akbari V, Wan Alwi SR, Manan ZA. CO 2 capture with potassium carbonate solutions: A state-of-the-art review. Int J Greenh Gas Control 2015;41:142–62. https://doi.org/10.1016/j.ijggc.2015.06.026.

[24] Hu G, Nicholas NJ, Smith KH, Mumford KA, Kentish SE, Stevens GW. Carbon dioxide absorption into promoted potassium carbonate solutions: A review. Int J Greenh Gas Control 2016;53:28–40. https://doi.org/https://doi.org/10.1016/j.ijggc.2016.07.020.

[25] Borhani TNG, Akbari V, Hamid MKA, Manan ZA. Rate-based simulation and comparison of various promoters for CO<inf>2</inf> capture in industrial DEA-promoted potassium carbonate absorption unit. J Ind Eng Chem 2015. https://doi.org/10.1016/j.jiec.2014.07.024.

[26] Bhosale RR, Kumar A, AlMomani F. Kinetics of reactive absorption of CO2 using aqueous blend of potassium carbonate, ethylaminoethanol, and N-methyl-2-Pyrollidone (APCEN solvent). J Taiwan Inst Chem Eng 2018;89:191–7. https://doi.org/https://doi.org/10.1016/j.jtice.2018.05.016.

[27] Mondal BK, Bandyopadhyay SS, Samanta AN. Equilibrium solubility and enthalpy of CO2 absorption in aqueous bis(3-aminopropyl) amine and its mixture with MEA, MDEA, AMP and K2CO3. Chem Eng Sci 2017;170:58–67. https://doi.org/https://doi.org/10.1016/j.ces.2017.01.040.

[28] Behr P, Maun A, Deutgen K, Tunnat A, Oeljeklaus G, Görner K. Kinetic study on promoted potassium carbonate solutions for CO2 capture from flue gas. Energy Procedia 2011;4:85–92. https://doi.org/http://dx.doi.org/10.1016/j.egypro.2011.01.027.

[29] Cullinane JT, Rochelle GT. Carbon dioxide absorption with aqueous potassium carbonate promoted by piperazine. Chem Eng Sci 2004;59:3619–30. https://doi.org/http://dx.doi.org/10.1016/j.ces.2004.03.029.

[30] Hilliard MD, Rochelle GT. Thermodynamics of aqueous piperazine/potassium carbonate/carbon dioxide chare cterized by the electrolyte non-random two-liquid model in aspen plus. In: Rubin ES, Keith DW, Gilboy CF, Wilson M, Morris T, Gale J, et al., editors. Greenh. Gas Control Technol. 7, Oxford: Elsevier Science Ltd; 2005, p. 1975–8. https://doi.org/http://dx.doi.org/10.1016/B978-008044704-9/50253-6.

[31] Cullinane JT, Rochelle GT. Kinetics of Carbon Dioxide Absorption into Aqueous Potassium Carbonate and Piperazine. Ind Eng Chem Res 2005;45:2531–45.

https://doi.org/10.1021/ie050230s.

[32] Tim Cullinane J, Oyenekan BA, Lu J, Rochelle GT. - Aqueous piperazine/potassium carbonate for enhanced CO2 capture. In: Rubin ES, Keith DW, Gilboy CF, Wilson M, Morris T, Gale J, et al., editors. Greenh. Gas Control Technol. 7, Oxford: Elsevier Science Ltd; 2005, p. 63–71. https://doi.org/https://doi.org/10.1016/B978-008044704-9/50008-2.

[33] Chen E. Carbon Dioxide Absorption into Piperazine Promoted Potassium Carbonate using Structured Packing. University of Texas at Austin, 2007.

[34] Krishnamurthy R, Taylor R. Simulation of packed distillation and absorption columns. Ind Eng Chem Process Des Dev 1985;24:513–24. https://doi.org/10.1021/i200030a001.

[35] Afkhamipour M, Mofarahi M. Comparison of rate-based and equilibrium-stage models of a packed column for post-combustion CO2 capture using 2-amino-2-methyl-1-propanol (AMP) solution. Int J Greenh Gas Control 2013;15:186–99. https://doi.org/http://dx.doi.org/10.1016/j.ijggc.2013.02.022.

[36] Bravo JL, Fair JR. Generalized correlation for mass transfer in packed distillation columns. Ind Eng Chem Process Des Dev 1982;21:162–70.

[37] Austgen DM, Rochelle GT, Peng X, Chen CC. Model of vapor-liquid equilibria for aqueous acid gas-alkanolamine systems using the electrolyte-NRTL equation. Ind Eng Chem Res 1989;28:1060–73. https://doi.org/10.1021/ie00091a028.

[38] Hetzer HB, Robinson RA, Bates RG. Dissociation constants of piperazinium ion and related thermodynamic quantities from 0 to 50. deg. J Phys Chem 1968;72:2081–6.

[39] Danckwerts PV. Gas-liquid reactions. New York: McGraw-Hill; 1970.

[40] Borhani TN, Nabavi SA, Hanak DP, Manovic V. Thermodynamic models applied to CO2 absorption modelling. Rev Chem Eng 2020.

[41] Chen CC, Britt HI, Boston JF, Evans LB. Local composition model for excess Gibbs energy of electrolyte systems. Part I: Single solvent, single completely dissociated electrolyte systems. AIChE J 1982;28:588–96. https://doi.org/10.1002/aic.690280410.

[42] Kenig EY, Schneider R, Górak A. Reactive absorption: Optimal process design via optimal modelling. Chem Eng Sci 2001;56:343–50. https://doi.org/https://doi.org/10.1016/S0009-2509(00)00234-7.

[43] Škrbić B, Cvejanov J. Liquid holdup determination in packed columns for sulfur dioxide absorption. Gas Sep Purif 1994;8:13–6. https://doi.org/https://doi.org/10.1016/0950-4214(94)85003-8.

[44] Stichlmair J, Bravo JL, Fair JR. General model for prediction of pressure drop and

capacity of countercurrent gas/liquid packed columns. Gas Sep Purif 1989;3:19–28. https://doi.org/http://dx.doi.org/10.1016/0950-4214(89)80016-7.

[45] Al-Rashed OA, Ali SH. Modeling the solubility of CO2 and H2S in DEA–MDEA alkanolamine solutions using the electrolyte–UNIQUAC model. Sep Purif Technol 2012;94:71–83. https://doi.org/http://dx.doi.org/10.1016/j.seppur.2012.04.007.

[46] Poling BE, Prausnitz JM, O'Connell JP. The Properties of Gases and Liquids 5E. McGraw-Hill Education; 2000.

[47] Thomsen K. Aqueous electrolytes: model parameters and process simulation, PhD Thesis. Technical University of Denmark, 1997.

[48] Sanyal D, Vasishtha N, Saraf DN. Modeling of carbon dioxide absorber using hot carbonate process. Ind Eng Chem Res 1988;27:2149–56. https://doi.org/10.1021/ie00083a032.

[49] Ooi SMP. Development and demonstration of a new non-equilibrium rate-based process model for the hot potassium carbonate process. 2009.

[50] Chung TH, Ajlan M, Lee LL, Starling KE. Generalized multiparameter correlation for nonpolar and polar fluid transport properties. Ind Eng Chem Res 1988;27:671–9. https://doi.org/10.1021/ie00076a024.

[51] Akbari V, Dehghani MR, Borhani TNG, Azarpour A. Activity Coefficient Modelling of Aqueous Solutions of Alkyl Ammonium Salts using the Extended UNIQUAC Model. J Solution Chem 2016. https://doi.org/10.1007/s10953-016-0510-x.

[52] Aseyev GG, Zaytsev ID. Volumetric Properties of Electrolyte Solutions: Estimation Methods and Experimental Data. Begell House New York; 1996.

[53] Puchkov L V, Kurochkina V V. Saturated vapor pressure over aqueous solutions of potassium carbonate. Zhur Priklad Khim 1970;43:181–3.

[54] Cullinane JT, Rochelle GT. Thermodynamics of aqueous potassium carbonate, piperazine, and carbon dioxide. Fluid Phase Equilib 2005;227:197–213. https://doi.org/http://dx.doi.org/10.1016/j.fluid.2004.11.011.

[55] Aseyev GG. Electrolytes: equilibria in solutions and phase equilibria. Begell House; 1999.

[56] Tosh JS. Equilibrium Study of the System Potassium Carbonate, Potassium Biocarbonate, Carbon Dioxide, and Water. vol. 5484. United States Bureau of Mines; 1959.

[57] Kamps ÁP-S, Xia J, Maurer G. Solubility of CO2 in (H2O+piperazine) and in (H2O+MDEA+piperazine). AIChE J 2003;49:2662–70.

https://doi.org/10.1002/aic.690491019.

[58] Bishnoi S. Carbon Dioxide Absorption and solution equilibrium in piperazine-activated methyldiethanolamine. The University of Texas at Austin; 2000.

[59] Hilliard M. A Predictive Thermodynamic Model for an Aqueous Blend of Potassium Carbonate, Piperazine, and Monoethanolamine for Carbon Dioxide Capture from Flue Gas. The University of Texas at Austin, 2008.

[60] Derks PWJ, Dijkstra HBS, Hogendoorn JA, Versteeg GF. Solubility of carbon dioxide in aqueous piperazine solutions. AIChE J 2005;51:2311–27. https://doi.org/10.1002/aic.10442.

[61] Ermatchkov V, Pérez-Salado Kamps Á, Maurer G. Chemical equilibrium constants for the formation of carbamates in (carbon dioxide+piperazine+water) from 1H-NMR-spectroscopy. J Chem Thermodyn 2003;35:1277–89. https://doi.org/https://doi.org/10.1016/S0021-9614(03)00076-4.

[62] Kim I. Heat of reaction and VLE of post combustion CO2 absorbents. Norges teknisk-naturvitenskapelige universitet, Fakultet for naturvitenskap …; 2009.

[63] Tosh JS, Field JH, Benson HE, Haynes WP. Equilibrium study of the system potassium carbonate, potassium bicarbonate, carbon dioxide, and water. 1959.

[64] Cullinane JT. Thermodynamics and Kinetics of Aqueous Piperazine with Potassium Carbonate for Carbon Dioxide Absorption. The University of Texas at Austin, 2005.

[65] Tontiwachwuthikul P, Meisen A, Lim CJ. CO2 absorption by NaOH, monoethanolamine and 2-amino-2-methyl-1-propanol solutions in a packed column. Chem Eng Sci 1992;47:381–90. https://doi.org/http://dx.doi.org/10.1016/0009-2509(92)80028-B.

[66] Afkhamipour M, Mofarahi M. Modeling and optimization of CO 2 capture using 4-diethylamino-2-butanol (DEAB) solution. Int J Greenh Gas Control 2016;49:24–33.

[67] Iliuta I, Larachi F. CO2 abatement in oscillating packed-bed scrubbers: Hydrodynamics and reaction performances for marine applications. AIChE J 2017;63:1064–76. https://doi.org/https://doi.org/10.1002/aic.15450.

[68] Zhang Y, Chen H, Chen C-C, Plaza JM, Dugas R, Rochelle GT. Rate-Based Process Modeling Study of CO2 Capture with Aqueous Monoethanolamine Solution. Ind Eng Chem Res 2009;48:9233–46. https://doi.org/10.1021/ie900068k.

[69] Faramarzi L, Kontogeorgis GM, Michelsen ML, Thomsen K, Stenby EH. Absorber Model for CO2 Capture by Monoethanolamine. Ind Eng Chem Res 2010;49:3751–9. https://doi.org/10.1021/ie901671f.

[70] Borhani TNG, Akbari V, Afkhamipour M, Hamid MKA, Manan ZA. Comparison of equilibrium and non-equilibrium models of a tray column for post-combustion CO2 capture using DEA-promoted potassium carbonate solution. Chem Eng Sci 2015. https://doi.org/10.1016/j.ces.2014.09.017.